

# A Preferential Attachment Model for the Initial Mass Function

Jessi Cisewski-Kehe\*

Department of Statistics and Data Science, Yale University

and

Grant Weller†

Savvysherp, Minneapolis, MN 55430

and

Chad Schafer

Department of Statistics and Data Science, Carnegie Mellon University

and

David W. Hogg

Center for Cosmology and Particle Physics, New York University

June 8, 2018

## Abstract

Accurate specification of a likelihood function is becoming increasingly difficult in many inference problems in astronomy. As the sample sizes resulting from astronomical surveys continue to grow, deficiencies in the likelihood function lead to larger biases in key parameter estimates. These deficiencies result from the oversimplification of the physical processes that generated the data, and from the failure to account for observational limitations. Unfortunately, realistic models often do not yield an analytical form for the likelihood. The estimation of a stellar initial mass function (IMF) is an important example. The stellar IMF is the mass distribution of stars initially formed in a given cluster of stars, a population which is not directly observable due to stellar evolution and other disruptions of the cluster. There are several difficulties with specifying a likelihood in this setting, since the physical processes and observational challenges result in measurable masses that cannot legitimately be considered independent draws from an IMF. This work improves inference of the

---

\*The authors gratefully acknowledge *please remember to list all relevant funding sources in the unblinded version*

†Corresponding author

IMF by using an approximate Bayesian computation approach that both accounts for observational and astrophysical effects and incorporates a physically-motivated model for star cluster formation. The methodology is illustrated via a simulation study, demonstrating that the proposed approach can recover the true posterior in realistic situations, and applied to observations from the Orion Nebula Cluster.

*Keywords:* Approximate Bayesian computation, astrostatistics, computational statistics, dependent data

## 1 Introduction

The Milky Way is home to billions of stars (McMillan 2016), many of which are members of *stellar clusters* - gravitationally bound collections of stars. Stellar clusters are formed from low temperature and high density clouds of gas and dust called *molecular clouds*, though there is uncertainty as to how the stars in a cluster form (Beccari et al. 2017). Each theory of star formation yields a different prediction for the distribution of the masses of stars that initially formed in a cluster. Hence, it is of fundamental interest to estimate this distribution, referred to as the *stellar initial mass function (IMF)*, and assess the validity of these competing theories. In fact, research advances in many areas of stellar, galactic, and extragalactic astronomy are at least somewhat reliant upon accurate understanding of the IMF (Bastian et al. 2010). For example, the IMF is a key component of galaxy and stellar evolution and planet formation (Bally & Reipurth 2005, Bastian et al. 2010, Shetty & Cappellari 2014), along with chemical enrichment and abundance of core-collapse supernovae (Weisz et al. 2013).

There is also ongoing discussion surrounding the *universality* of the IMF, i.e., if a single IMF describes the generative distribution of stellar masses for all star clusters (Bastian et al. 2010). Even though the consensus of the astronomical community is that there is a universal IMF, most of the observations had been consistent with universality. With further research and growing sample sizes, however, there is increased theoretical (Dib et al. 2010, Bonnell et al. 2006) and observational (Treu et al. 2010, Spiniello et al. 2014, Dib et al. 2017, Geha et al. 2013) support for an IMF that varies from cluster to cluster.

Salpeter (1955) studied the evolutionary properties of certain populations of stars, and in the process defined the first IMF (which he called the “original mass function”). This work put forth the now-classic model for the IMF, a power law with a finite upper bound equal to the physical maximum mass of a star that could form in a cluster (Salpeter 1955). Recent studies support the validity of this power law form for the IMF for stars of mass greater than half that of our sun (Massey 2003, Bastian et al. 2010, Lim et al. 2013).

**JESSI: CHECK PREVIOUS CLAIM.** Similar models have been proposed and used in the astronomical literature for inference of the stellar initial mass function; these will be discussed in the next section. The estimation of the parameters of these proposed models typically relies on the unphysical assumption that the observed stars in a stellar cluster form independently. This work loosens this restriction in order to explore one of several possible physical formation mechanisms of cluster formation (Li et al. 2017).

Despite this seemingly simple form of the power law model, the statistical challenges of estimating the IMF using *observed* stars from a cluster are significant. Many of the limitations are related to observational issues and to the adequate modeling of the evolution of a star cluster after the initial formation. For example, since stars of greater mass die more rapidly, the upper tail of the IMF is not observed in a cluster of sufficient age. Also, the death of massive stars can trigger additional star formation, contaminating the lower end of the IMF with new stars (Woosley & Heger 2015).

The observational limitations and the challenge of modeling cluster evolution make *approximate Bayesian computation (ABC)* appealing for estimation of the IMF, as ABC allows for relatively easy incorporation of such effects. In particular, a primary appeal of ABC for this application is the ability to incorporate more complex models for cluster formation. Standard IMF models do not specify the process by which a large mass of gas (the molecular cloud) transforms into a gravitationally bound collection of stars. ABC is based on a simple rejection-sampling approach, in which draws of model parameters from a prior distribution are fed through a simulation model to generate a sample of data. If the generated sample is “close” (based on an appropriately chosen metric) to the observed data, the prior draw that produced that generated sample is retained. The collection of

accepted parameter values comprise draws from an approximation to the posterior. The simulations (the *forward model*) can include any of the complex processes that make it challenging to derive a likelihood function for the observable data.

Hence, with the goal of improving inference on the IMF by incorporating effects that are often otherwise ignored (Kalari et al. 2018, Ashworth et al. 2017, Jose et al. 2017), **THIS IS A VERY IMPORTANT POINT. THESE REFERENCES SHOULD BE CHECKED, AND MAYBE MORE ADDED.** along with connecting a possible formation mechanism with the IMF, an ABC approach is described in this work. This situation is typical of inference challenges that arise in astronomy. See Schafer & Freeman (2012), Akeret et al. (2015), Ishida et al. (2015) for reviews. Recent years have seen a rapid increase in the use of ABC methods for estimation in this field, including specific application to Milky way properties (Robin et al. 2014), strong lensing of galaxies (Killedar et al. 2018, Birrer et al. 2017), large scale structure of the Universe (Hahn, Vakili, Walsh, Hearin, Hogg & Campbell 2017), estimating the redshift distribution (Herbel et al. 2017), galaxy evolution (Hahn, Tinker & Wetzel 2017), weak lensing (Peel et al. 2017, Lin & Kilbinger 2015), exoplanets (Parker 2015), galaxy morphology (Cameron & Pettitt 2012), and supernovae (Weyant et al. 2013).

This paper is organized as follows. In Section 2 we will present background on the IMF along with inference challenges, and introduce ABC. We propose a new stochastic model for stellar formation in Section 3 and discuss our ABC procedure. Section ?? applies the proposed methodology to the estimation of the IMF of the Orion Nebular Cluster, using a recent sample of observations from this scientifically-important Milky Way cluster (Hillenbrand & Hartmann 1998, Da Rio et al. 2012). Finally, Section 5 provides a discussion.

## 2 Background

### 2.1 Stellar Initial Mass Function

As noted above, Salpeter (1955) introduced the power law model for the shape of the IMF for masses larger than  $0.5M_{\odot}$ , where  $M_{\odot}$  is the mass of the Sun. Kroupa (2001) extended the range of the IMF by proposing a three-part broken power law model over the range

$0.01M_{\odot} < m < M_{max}$ , where  $M_{max}$  is the mass of the largest star that could form with nonzero probability. This model postulates different forms for the IMF for stars of masses  $0.01M_{\odot} < m < 0.08M_{\odot}$ ,  $0.08M_{\odot} < m < 0.5$  and  $m > 0.5M_{\odot}$ . Focusing on the upper part, and defining  $\theta = (\alpha, M_{max})$ , the probability density function for mass  $x$  in the upper tail of the stellar IMF is assumed to be given by

$$f_M(m | \theta) = cm^{-\alpha}, \quad m \in [M_{min}, M_{max}], \quad (1)$$

where the constant  $c$  is chosen such that  $f_M$  is a valid probability density. Alternative models have been proposed that include log-normal distributions, joint power law and log-normal parts, and truncated exponential distributions (Chabrier 2005, Offner et al. 2014). The Kroupa (2001) and Chabrier (2005) models are displayed in Figure 1 along with observational challenges discussed §2.1.1. Power law distributions and log-normal distributions are closely related and may be the result of subtle differences in the underlying formation mechanism (Mitzenmacher 2004). The IMF model we propose will exploit one possible underlying formation mechanism that we show results in power law tails.

### 2.1.1 Observational Challenges

Observing all stars comprising an IMF is not feasible, as the most massive stars ( $m > 10M_{\odot}$ ) have lifetimes of only a few million years. The lifetime of a star (the time it takes for the star to burn through its hydrogen) depends strongly on its mass: the most massive stars have shorter lives due to the hotter temperatures they must maintain to avoid collapse from the strong gravitational forces. In particular, stellar life is approximately proportional to  $m^{-\rho}$  where  $\rho \approx 3$  (Hansen et al. 2004, p. 30, Chaisson & McMillan 2011, p. 439). Hence, the mass of the largest star observed in a given cluster depends on the cluster age.

Furthermore, the IMF will be estimated using a noisy, incomplete view of that cluster. Whether or not a star is observed is dependent on several factors including its mass, its location in the cluster, and its neighbors. Some of these factors are described by a data set's *completeness function*, which quantifies a given star's probability of being observed. This depends on its luminosity (i.e. intrinsic brightness) since it needs to be sufficiently bright to be observable; in particular, completeness depends on stellar flux in comparison

with the flux limits of the observations. There are also issues with *mass segregation*: stars with lower mass tend to be on the edge of the cluster, while the most massive stars are often found in the center (Weisz et al. 2013). Due to *stellar crowding* in the center, stars in this region can be more difficult to observe. Additionally, binary stars (star systems consisting of a pair of stars) are difficult to distinguish from a single star, creating the potential for overstating the mass of an object and understating the number of stars in the cluster.

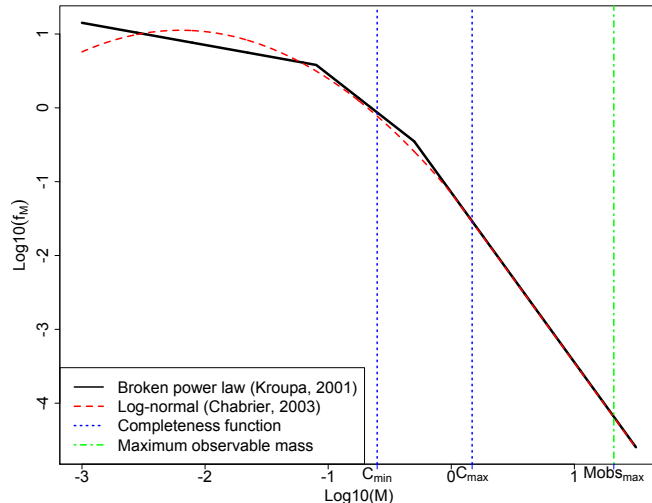


*Figure 1:* The broken power law model of Kroupa (2001) (black, line) and the lognormal model of Chabrier (2005) (red, dashed) are displayed along with vertical lines representing several observational challenges. The blue vertical dotted lines indicate the range of values ( $C_{\min}, C_{\max}$ ) on which the completeness function may be defined, and the vertical green dotted and dashed line indicates the maximum observable mass ( $M_{\text{obs},\max}$ ) due to the aging cutoff. The observational challenges are discussed further in §3.2.

There are additional uncertainties involved in translating the actual observables (e.g. photometric magnitudes) into a mass measurement; that is, the mass values for observable stars are only estimates. The *Hertzsprung-Russell (H-R) Diagram* is a classic visual summary of the distribution of the luminosity and temperature of a collection of stars. A typical H-R Diagram includes a *main sequence* of stars that trace a line from bright and hot stars to dim and cool stars. Stellar mass also evolves along this one-dimensional feature, and since luminosity and temperature are estimable, mass can thus also be estimated. The

mass of binary stars can be determined via Kepler’s Laws, and hence a *mass-luminosity relationship* can be fit to binaries and then extended to other stars on the main sequence. Unfortunately, luminosity and temperature are nontrivial to estimate, as corrections for effects such as *accretion* and *extinction* are required, along with an accurate estimate of the distance to the stars (Da Rio et al. 2010). The process is further complicated by the dependence of how these transformations are made on the *spectral type* of the star. Careful budgeting of the errors that accumulate is required in order to produce a reasonable error bars on mass estimates; Da Rio et al. (2010) utilize a Monte Carlo approach in which the errors in magnitudes are propagated forward through to uncertainties in the spectral type, the accretion and reddening corrections, and finally to an uncertainty on the mass.

## 2.2 Approximate Bayesian Computation

Standard approaches to Bayesian inference, either analytical or built on MCMC, require the specification of a likelihood function,  $f(m | \boldsymbol{\theta})$ , with data  $m_{\text{obs}} \in \mathcal{D}$ , and parameter(s)  $\boldsymbol{\theta} \in \Theta$ . In many modern scientific inference problems, such as for some emerging models for the stellar IMF, the likelihood is too complicated to be derived or otherwise specified. As noted previously, ABC provides an approximation to the posterior without specifying a likelihood function, and instead relies on forward simulation of the data generating process.

The basic algorithm for sampling from the ABC posterior is attributed to Tavaré et al. (1997) and Pritchard et al. (1999), used for applications to population genetics. The algorithm has three main steps which are repeated until a sufficiently large sample is generated: *Step 1*, Sample  $\boldsymbol{\theta}^*$  from the prior; *Step 2*, Generate  $m_{\text{sim}}$  from forward process assuming truth  $\boldsymbol{\theta}^*$ ; *Step 3*, Accept  $\boldsymbol{\theta}^*$  if some distance function  $\rho(m_{\text{obs}}, m_{\text{sim}}) \leq \epsilon$ , where  $\epsilon$  is a tuning parameter that should be close to 0. This last step typically consists of comparing low-dimensional summary statistics generated for the observed and simulated datasets. Adequate statistical and computational performance of ABC algorithms depends greatly on the selection of such summary statistics (Joyce & Marjoram 2008, Blum & François 2010, Blum 2010, Fearnhead & Prangle 2012, Blum et al. 2013).

The basic ABC algorithm can be inefficient in cases where the parameter space is of

moderate or high dimension. Hence, important adaptations of the basic ABC algorithm incorporate ideas of sequential Monte Carlo (SMC) in order to improve the sampling efficiency (Marjoram et al. 2003, Sisson et al. 2007, Beaumont et al. 2009, Del Moral et al. 2011). A nice overview of ABC can be found in Marin et al. (2012). Here, we use a sequence of decreasing tolerances  $\epsilon_{1:T} = (\epsilon_1, \dots, \epsilon_T)$  with the tolerance  $\epsilon_t$  shrinking until further reductions do not significantly affect the resulting ABC posterior. The improvement in efficiency is due to the modification that happens after the first time step: instead of sampling from the prior distribution, the proposed  $\boldsymbol{\theta}$  are drawn from the previous time step’s ABC posterior. Using this adaptive proposal distribution can help to improve the sampling efficiency. The resulting draws, however, are not targeting the correct posterior, and so importance weights,  $W_t$ , are used to correct this discrepancy.

### 3 Forward Model for the IMF

Due to their simple interpretations, mathematical ease, and demonstrated consistency with observations, power law IMFs (or similar variants) have been widely adopted in the astronomy literature (Kroupa et al. 2012); however, open questions remain about stellar formation processes. The proposed forward model is a way to link a possible stellar formation process with the realized mass function (MF). One known underlying mechanism for producing data with power-law tails is based on *preferential attachment* (PA). The earliest PA model, the Yule-Simon process, was popularized by Simon (1955), and was originally used to model biological genera and word frequencies. **ADD OTHER USES.** In the stellar formation context, linear PA models generate power law IMFs; sublinear variants produce slight deviations from power laws, and exponential cutoffs can also be induced.

add discussion about PA model, and nonlinear attachment. Proof of power law tails. Use in networks. We need to generalize.

#### 3.1 Preferential attachment for the IMF

describe formation theory we are going to try to capture. Rather than assuming that stellar masses in a cluster arise independently of each other, our PA model proposes a resource-limited mass accretion process between stellar cores whose ability to accumulate additional mass is a function of their existing masses. This dependence feature is particularly important for statistical inference, as models that assume independent observations of stellar masses are vulnerable to incorrect and misleading inference. Additionally, the mass of the largest star to form in a cluster is limited by the total cluster mass.

Our proposed stochastic model for stellar formation is as follows: we first fix a total available cluster mass  $M_{\text{tot}}$ . This quantity can be physically interpreted as the total mass available for stellar formation in a molecular cloud. At each time step  $t = 1, 2, \dots$ , a random quantity of mass  $m_t \sim \text{Exponential}(\lambda)$  enters the collection of stars;  $M_{1,1} = m_1$  becomes the mass of the first star. Subsequent masses entering the system form a new star with probability  $\pi_t$  or join existing star  $k = 1, \dots, n_t$  with probability  $\pi_{kt}$ . These probabilities are specified as

$$\pi_t = \min(1, \alpha) \quad \text{and} \quad \pi_{kt} \propto M_{k,t}^\gamma. \quad (2)$$

The generating process is complete when the total mass of formed stars reaches  $M_{\text{tot}}$ . The possible ranges of the five parameters are  $\lambda > 0$ ,  $\alpha \in [0, 1]$ , and  $\gamma > 0$ .

**Proof of power law tails???** Put in appendix.

The parameter  $\alpha$  defines the probability that entering mass forms a new star in a cluster. For the growth component, the model allows for linear ( $\gamma = 1$ ), sublinear ( $\gamma < 1$ ), and superlinear ( $\gamma > 1$ ) behavior; the limiting case of  $\gamma \rightarrow 0$  gives a uniform attachment model. Finally, the parameter  $\lambda$  acts as a scaling factor which controls the average ‘coarseness’ of masses joining the forming stellar cores.

The proposed PA mass generation model offers considerable flexibility to approximate existing IMF models in the literature. In Figure 2, IMF realizations were drawn assuming the Kroupa (2001) broken power-law model as the truth model and the Chabrier (2005) lognormal model as the true model. Our proposed PA ABC procedure was then used for inference and captures the general shape of the true model.

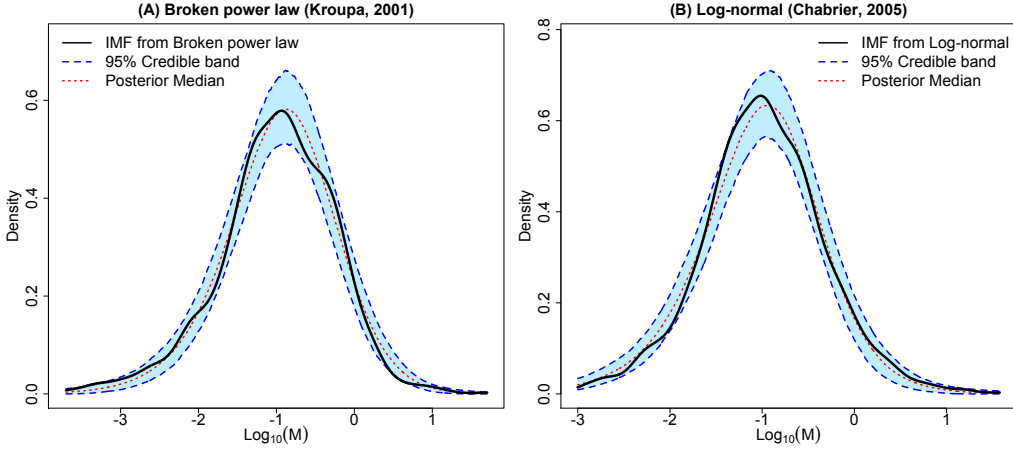


*Figure 2:* The solid black lines display the IMF with 1,000 stars drawn from (A) the broken power-law model of Kroupa (2001) and (B) the log-normal model of Chabrier (2005). The proposed PA ABC model was used with  $N = 1,000$  particles, and 95% point-wise credible bands are displayed (blue, dashed lines) along with the posterior median (red, dotted) for each data set. The preferential attachment model provides flexibility to approximate both existing models.

### 3.2 Initial Mass Function to the Observed Mass Function

The PA model describes the formation of a star cluster at initial formation. However, we are not generally able to observe the star cluster after initial formation due to observational uncertainties, measurement uncertainties, and aging and dynamical evolution of the cluster. A cluster’s present-day observed mass function (MF) is the observed distribution of the stellar masses of a particular cluster.

Observation limitations can be easily incorporated into the ABC framework. For simplicity, we adopt a “linear ramp” completeness function describing the probability of observing a star of mass  $m$ :

$$\Pr(\text{observing a star} \mid m) = \begin{cases} 0, & m < C_{\min} \\ \frac{m-C_{\min}}{C_{\max}-C_{\min}}, & m \in [C_{\min}, C_{\max}] \\ 1, & m > C_{\max}. \end{cases} \quad (3)$$

We assume that the values  $C_{\min}$  and  $C_{\max}$  are known, though we note that selecting an

appropriate completeness function is a difficult process which requires quantification from the observational astronomers for each set of data. Different models for the completeness function could also be considered, including those which allow for spatially-varying observational completeness. A benefit of ABC is the ease at which a new completeness function can be incorporated – it amounts to a simple change in the forward model.

Due to measurement error and practical limitations in translating luminosities into masses, the masses of stars are not perfectly known. This uncertainty can be incorporated in different ways; following Weisz et al. (2013), we assume that the inferred mass of a star  $m_i$  is related to its true mass  $M_i$  via

$$\log m_i = \log M_i + \sigma_i \eta_i, \quad (4)$$

where  $\eta_i$  is a standard normal random variable, and  $\sigma_i$  is known measurement error. The model for mass uncertainties in (4) is simple and could be extended to account for other sources of uncertainty (e.g. redshift).

As noted previously, the lifecycle of a star depends on certain characteristics such as mass. In the proposed algorithm, stars generated in a cluster are aged using a simple truncation of the largest masses. That is, the distribution of stellar masses for a star cluster of age  $\tau$  Myr is given by

$$f_M(m | \theta, \tau) = f_M(m | \theta) \mathbb{I}\{M \leq \tau^{-1/3} \times 10^{4/3}\}, \quad (5)$$

corresponding to stellar lifetimes of  $10^4 M^{-3}$  Myr, where  $M$  is the mass of the star (Hansen et al. 2004, Chaisson & McMillan 2011). More sophisticated models that account for effects such as binary stars and stellar wind mass loss can be inserted into this framework.

## 4 Methods

We propose an ABC framework to make inferences on the IMF given a cluster’s present-day observed MF. The proposed ABC algorithm is displayed in Algorithm (1), where  $N$  is the desired particle sample size to approximate the posterior distribution, and is motivated by the adaptive ABC algorithm of Beaumont et al. (2009). The forward model,  $F$ , in

Algorithm (1) is where observational limitations and uncertainties, stellar evolution, and other astrophysical elements can be incorporated as outlined in Section 3.

Algorithm (1) is initialized using the basic ABC rejection algorithm at time step  $t = 1$  using a distance function  $\rho(m_{\text{sim}}, m_{\text{obs}})$  to measure the distance between the simulated and observed datasets,  $m_{\text{sim}}$  and  $m_{\text{obs}}$ , respectively. The first tolerance,  $\epsilon_1$ , is adaptively selected by drawing  $kN$  particles for some  $k > 0$ . Then the  $N$  particles that have the smallest distance are retained, and  $\epsilon_1$  is defined as the largest of those  $N$  distances retained. For subsequent time steps ( $t > 1$ ), rather than proposing a draw,  $\theta^*$ , from the prior,  $\pi(\theta)$ , the proposed  $\theta^*$  is selected from the previous time step's ( $t - 1$ ) ABC posterior samples. The selected  $\theta^*$  is then moved according to some kernel,  $K(\theta^*, \cdot)$ , to ameliorate degeneracy as the sampler evolves. In order to ensure the true posterior (which requires sampling from the prior) is targeted, the retained draws are weighted according to the appropriate importance weights,  $W_t$  – this incorporates the proposal distribution's kernel.

A key step in the implementation of an ABC algorithm is to quantify the distance between the simulated and observed stellar masses. We define a bivariate summary statistic and distance function that captures the shape of the present-day MF and the random number of stars observed, displayed in Equations (6) and (7), respectively. For the shape of the present-day MF, we use a kernel density estimate of the  $\log_{10}$  masses (due to the heavy-tailed distribution of the initial masses), and an  $L_2$  distance between the simulated and observed  $\log_{10}$  mass function estimates. The number of stars observed is the other summary statistic, with the distance being the absolute value of the difference in the ratio of the counts from 1. The bivariate summary statistic is defined as

$$\rho_1(m_{\text{sim}}, m_{\text{obs}}) = \left[ \int \left\{ \hat{f}_{\log m_{\text{sim}}}(x) - \hat{f}_{\log m_{\text{obs}}}(x) \right\}^2 dx \right]^{1/2} \quad (6)$$

$$\rho_2(m_{\text{sim}}, m_{\text{obs}}) = \max \left\{ \left| 1 - n_{\text{sim}}/n_{\text{obs}} \right|, \left| 1 - n_{\text{obs}}/n_{\text{sim}} \right| \right\}, \quad (7)$$

where the  $\hat{f}$  are kernel density estimates, and  $n_{\text{sim}}$  and  $n_{\text{obs}}$  are the number of stars comprising the observed MF. These summary statistics were selected based on performance of a simulation study using the high-mass section of the broken power-law model because the true posterior is known in this setting. Results and additional discussion of the simulation

study can be found in Appendix A.

With the bivariate summary statistic, we use a bivariate tolerance sequence,  $(\epsilon_{1t}, \epsilon_{2t})$ , for  $t = 1, \dots, T$  is such that  $\epsilon_{i1} \geq \epsilon_{i2} \geq \dots \geq \epsilon_{iT}$  for  $i = 1, 2$ . At time step  $t$ , the tolerances are determined based on the empirical distribution of the retained distances from time step  $t - 1$  (e.g. the 25th percentile). As noted previously, the tolerance sequence is initialized adaptively by selecting  $kN$  proposals from the prior distributions, then the  $N$  proposals that result in the  $N$  smallest distances were selected.<sup>1</sup>

In practice,  $M_{\text{tot}}$  is an unknown quantity of interest. A prior can be assigned to  $M_{\text{tot}}$  and an additional summary statistic and tolerance sequence can be used. The summary statistics we select in this case is

$$\rho_3(m_{\text{sim}}, m_{\text{obs}}) = \left| \sum_{i=1}^{n_{\text{sim}}} m_{\text{sim},i} - \sum_{j=1}^{n_{\text{obs}}} m_{\text{obs},j} \right|, \quad (8)$$

where  $m_{\text{sim},i}$  and  $m_{\text{obs},j}$  are the masses of the individual simulated and observed stars, respectively.

A short simulation study was carried out to illustrate the performance of the proposed model in the case where the solution is known, using the summary statistics in Equations (6)-(8). Values for the parameters  $(\lambda^{-1}, \alpha, \gamma, M_{\text{tot}})$  are displayed in Table 1 along with the number of stars produced,  $n_{\text{obs}}$ , which are used in the simulation as the observations. The generated IMF's used as the observations for each setting are displayed in Figure 3; number counts rather than densities are displayed in order to emphasize the different number of stars produced under each setting.

One of the more notable differences in the simulated IMFs displayed in Figure 3 used as the observations in the simulation study is the number of stars generated. The  $\alpha$  parameter controls the numbers stars that form and so there appears to be two groups of IMFs: one with  $\alpha = 0.3$  and one with  $\alpha = 0.7$ . The resulting marginal ABC posteriors for  $\lambda^{-1}$ ,  $\alpha$ ,  $\gamma$ , and  $M_{\text{tot}}$  are displayed in Figure 4. For  $\lambda^{-1}$  and  $M_{\text{tot}}$  (Figure 3(A) and (D), respectively) cover the input values well with differences in the width of the ABC posteriors. In general, the marginal ABC posteriors for  $\alpha$  and  $\gamma$  (Figure 3(B) and (C), respectively) cover the

---

<sup>1</sup>The  $kN$  sampled distances were scaled, squared, and then added together; the  $N$  smallest of these combined distances were retained.

input values of the parameters, but their shapes and widths vary. For example, the width of the marginal posteriors for  $\alpha$  appear to depend on the corresponding value of  $\gamma$ , where  $\gamma = 0.5$  results in the broadest marginal ABC posteriors for a fixed  $\alpha$ , and  $\gamma = 1.5$  results in the narrowest marginal ABC posteriors for a fixed  $\alpha$ . [[Jessi: I need to think more about why the previous statement happens]]

The pattern for  $\gamma$  is a bit more complicated. For a  $\gamma \leq 1$ , a smaller  $\alpha$  corresponds with a narrower posterior. This makes sense because a smaller  $\alpha$  results in fewer new stars, which means the entering piece of mass has to join an already formed star, at a rate controlled by the value of  $\gamma$ . Hence, more pieces that have to be assigned to existing stars seems to result in more information about the rate of growth of the stars. However, for a  $\gamma > 1$ , a larger  $\alpha$  (producing more new stars) appears to lead to a narrower marginal ABC posterior for  $\gamma$  than when  $\alpha$  is larger (0.7). The marginal ABC posterior for  $\gamma$  corresponding to the smaller value for  $\alpha$  (0.3) is wider and pushes against the boundary of the prior. Interestingly, it turns out that this behavior seems to occur because when  $\gamma$  is greater than 1 and  $\alpha$  is smaller, all the mass that has to be distributed to the already existing stars (rather than forming a new star) tends to be assigned to the same, most massive star. There ends up a being a runaway effect in the scenario with  $\gamma > 1$  and smaller  $\alpha$  where almost all of the incoming mass is assigned to the same star, resulting in one extremely massive star. This means there is essentially only one star for providing information on the  $\gamma$ , which may be why the ABC posterior is wider and pushes against the upper boundary of the prior on  $\gamma$ .

## 4.1 Astrophysical simulation data

Next we consider a star cluster generated from a radiation hydrodynamical simulation presented in Bate (2012). This simulation results in 183 stars and brown dwarfs formed from a  $500 M_{\odot}$  molecular cloud of uniform density, along with the growth of the stars and brown dwarfs across the duration of the simulation. Figure 6 displays the growth curves of the 183 objects and the IMF. The total mass of the resulting objects is about  $88.68 M_{\odot}$ . The details of the simulation can be found in Bate (2012). Validation of the simulated cluster was carried out by comparing the simulated cluster with real observations using

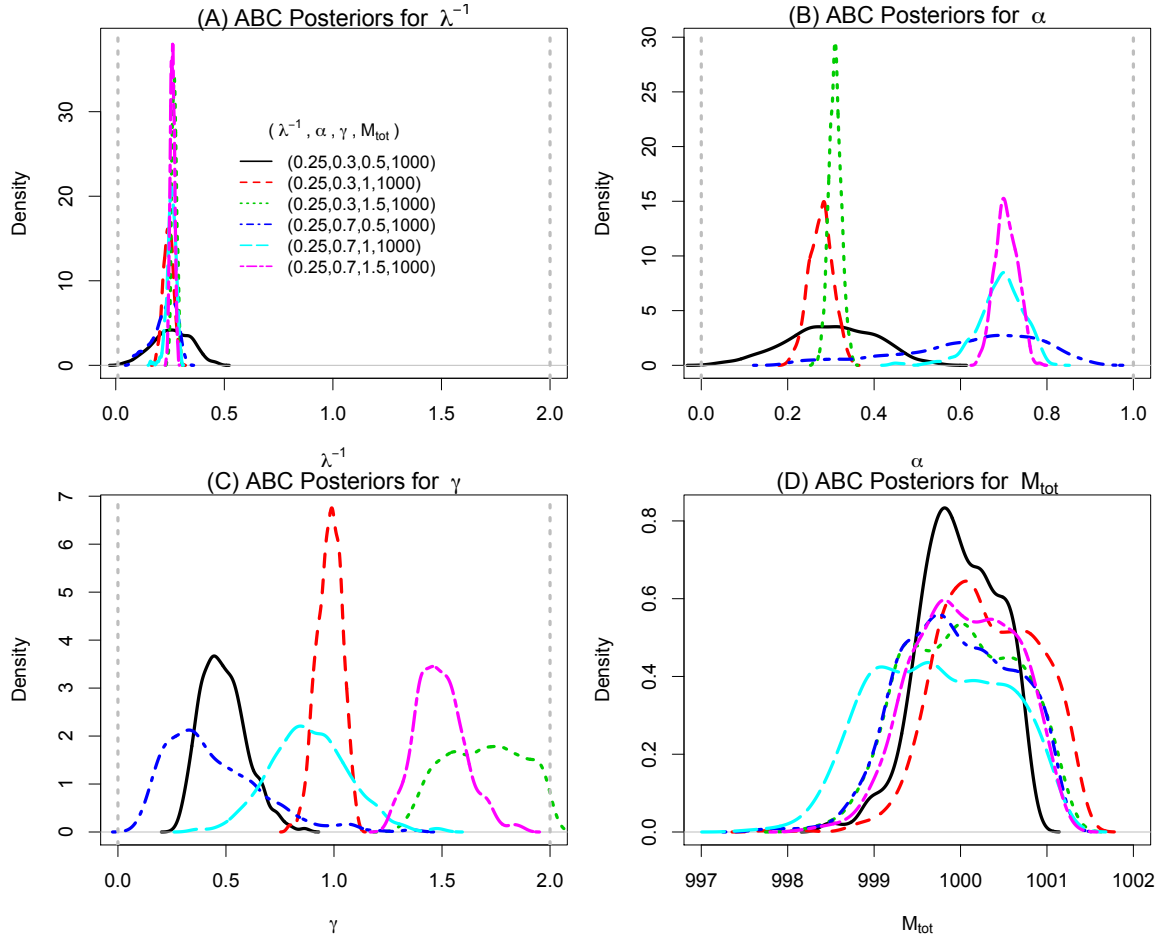


*Figure 4: Marginal ABC posteriors for the simulation settings of Table 1. The different color and types of lines indicate the input parameter values corresponding to the weighted kernel density estimates of the marginal ABC posteriors for (A)  $\lambda^{-1}$ , (B)  $\alpha$ , (C)  $\gamma$ , and (D)  $M_{\text{tot}}$ . The vertical dotted gray lines in plots (A) - (C) indicate the range of the uniform prior for the parameter. The prior used for  $M_{\text{tot}}$  was a Normal distribution with a prior mean of 1200 and a prior standard deviation of 600.*

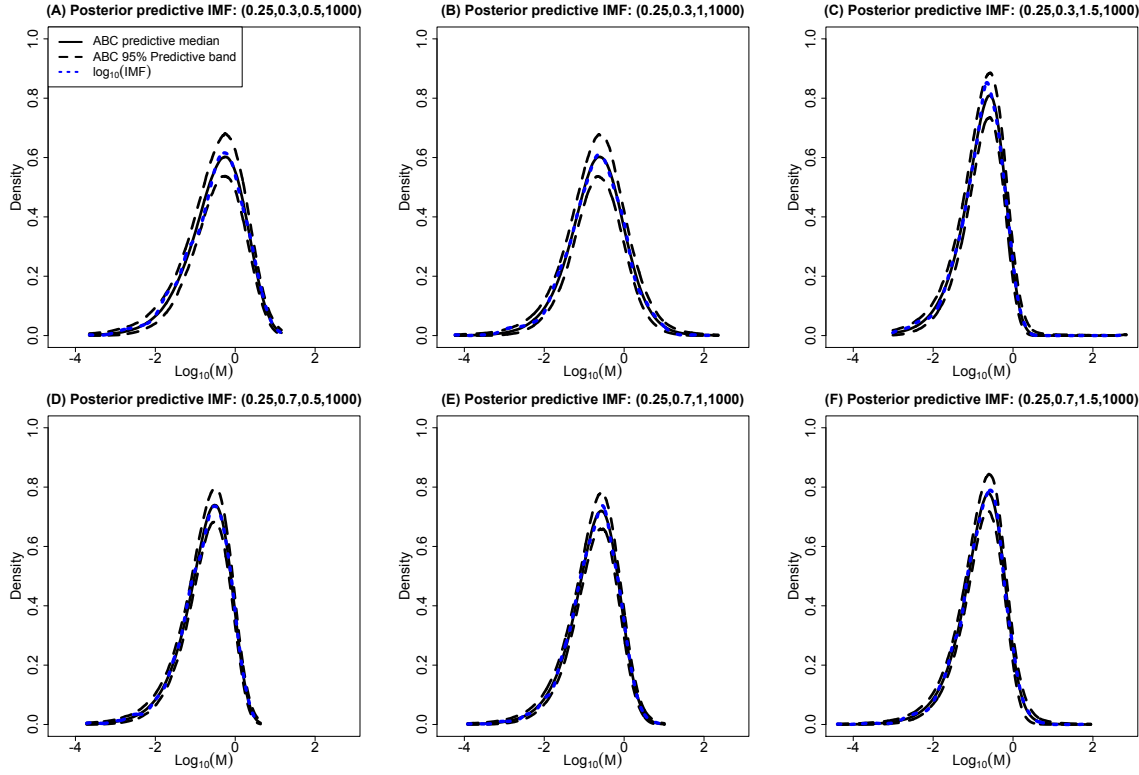


*Figure 5: ABC posterior predictive IMFs for the simulation settings of Table 1. The blue dotted lines display the true IMF used in each simulation setting, the solid black line is the median ABC posterior predictive IMF, and the dashed black lines indicate a point-wise 95% credible band. The posterior predictive IMFs and band were derived from taking 1000 draws from the final ABC posteriors in each setting, and then simulating an IMF using the sampled values. The input parameter values,  $(\lambda^{-1}, \alpha, \gamma, M_{tot})$ , are displayed in each sub-plot title.*

[ADD CLUSTER COMPARISONS MADE].

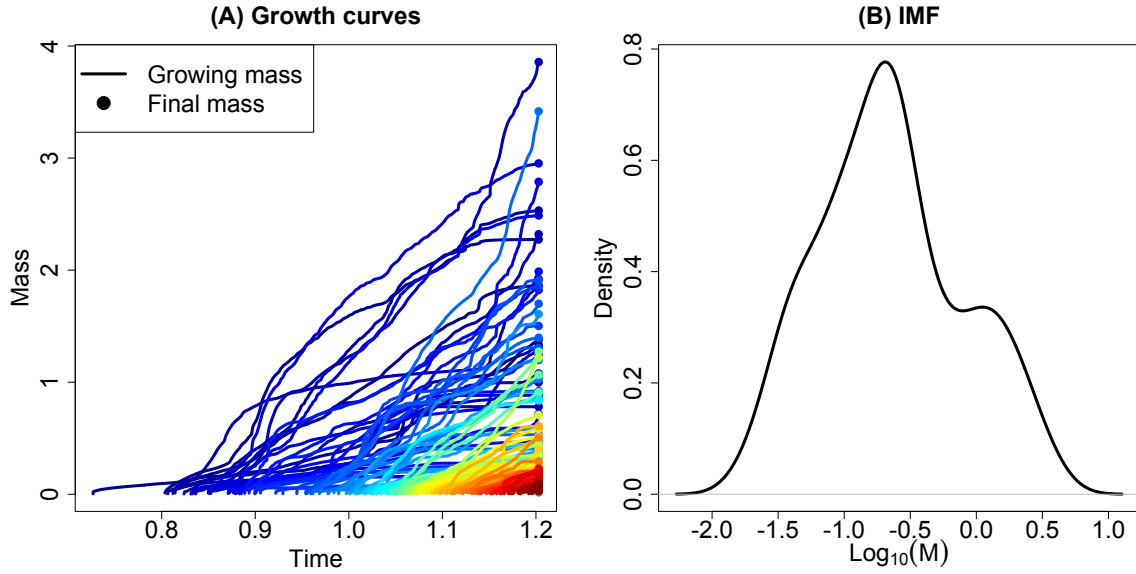


*Figure 6: Astrophysical simulation data. (A) The growth of stars and brown dwarfs across simulation time from Bate (2012), and (B) the resulting IMF. The colors in (A) distinguish the 183 stars and brown dwarfs.*

- Section 2.1 of Bate on sink particles seems to describe the accretion process
- In Bate - should not have significant super-linear attachment. Check to see if he has examples where there is super-linear attachment.

“Sink particles are permitted to merge in the calculation if they passed within 0.01 au of each other. However, no mergers occurred during the calculation.”

- 2.3.2 has discussion about the accretion radius
- Changes in the number of stars and mean masses with vs. without radiative feedback
- “In this paper, we refer to the mass function as an IMF because we compare it to the observed IMF since the PMF cannot yet be determined observationally. However, it should be noted that how a PMF transforms into the IMF depends on the accretion history of the protostars and how the star formation process is terminated.”

## 5 Discussion

Accounting for complex dependencies in observations, such as the initial masses of stars forming from a molecular cloud, is a challenging statistical problem. A possible, but unsatisfactory, resolution is simply to proceed as though the dependency is weak enough to assume independence. Instead, we draw from ideas in the preferential attachment literature proposing a new forward model to be used in an ABC algorithm. Though the new generative model was motivated by inference on stellar IMFs, it is generalizable to other applications that operate on a similar principle of dependent data. First we verified that the ABC approach works under the simplifying assumption of independence to ensure the true posterior was recoverable using ABC with the various observational effects. Then we introduced the new generative model, which starts with the total mass and stochastically builds individual stars of particular mass. The new model is general in the sense that it captures the dependencies among the masses of the stars, and also can accommodate standard models proposed in the astronomical literature.

The ONC is an interesting object of study among astronomers. The proposed preferential attachment model fitted via ABC captures the fluctuations in the observed mass function, as well as accounting for varying uncertainty as a function of available data in different regions of the mass range. While the proposed model is able to account for the dependency among the masses (along with the aging, completeness function, and observation uncertainty effects), it would be scientifically and statistically interesting to generalize the generative model to capture the spatial dependency among the observations. Intuitively, such an approach could account for a mechanism that limits the formation of multiple very massive stars relatively near to each other. Understanding the spatial distribution of masses of stars during formation would help advance our understanding stellar formation and evolution. Additionally, we did not attempt to capture the possible disturbances to the observed mass function as stars die, with the exception of deaths of the most massive stars.

Overall, the proposed generative model and ABC methodology provide a useful framework for dealing with complex physical processes that are otherwise difficult to work with

in a statistically rigorous fashion. As increasing computational resources allow for greater model complexity in studies of astronomy and other scientific fields, the proposed and other ABC algorithms may open new opportunities for Bayesian inference in challenging problems.

## A ABC summary statistic selection

In order to select effective summary statistics for the proposed model, we first employ the ABC methodology in a simplified study that focuses on the posterior of the power law parameter  $\alpha$  from Equation (1). We generate a cluster of  $n = 10^3$  stars from an IMF with slope  $\alpha = 2.35$  (Salpeter 1955),  $M_{min} = 2$ , and  $M_{max} = 60$ , a uniform prior distribution for  $\alpha \in (0, 6)$ , and with  $M_{max}$  considered known. This simple model was used in order to check the method against the true posterior of  $\alpha$  after the observational and aging effects have been incorporated into the forward model. We use the bivariate summary statistic and distance function of Equation (6). Defining the two-dimensional tolerance sequence as  $(\epsilon_{1t}, \epsilon_{2t})$  where the subscript  $t$  indicates the algorithm time step, and  $\epsilon_{11}$  and  $\epsilon_{21}$  were selected using an adaptive started discussed in Section 4 using an initial number of draws of  $10 \times N$  with  $N = 10^3$ . The algorithm ran for  $T = 5$  time steps. At steps  $t = 2, \dots, T$ ,  $\epsilon_{1t}$  and  $\epsilon_{2t}$  were set equal to the 25th percentile of the distances retained at the previous step from their corresponding distance functions.

The pseudo-data were aged 30 Myrs with the measurement error of  $\sigma = 0.25$  and observation completeness defined by the linear-ramp function in (3). Figure 7 displays the ABC posterior resulting from the ABC algorithm along with the true posterior for  $\alpha$ . The

ABC posterior matches the true posterior, defined as

$$\begin{aligned} \pi_F(\alpha \mid m_{\text{obs}}, M_{\min}, M_{\max}, n_{\text{obs}}, n_{\text{tot}}, T_{\text{age}}) &\propto \\ &\left\{ \Pr(M > T_{\text{age}}) + \left( \frac{1-\alpha}{M_{\max}^{1-\alpha} - M_{\min}^{1-\alpha}} \right) \int_2^4 M^{-\alpha} \left( 1 - \frac{M-2}{2} \right) dM \right\}^{n_{\text{tot}}-n_{\text{obs}}} \\ &\times \prod_{i=1}^{n_{\text{obs}}} \left\{ \int_2^{T_{\text{age}}} (2\pi\sigma^2)^{-\frac{1}{2}} m_i^{-1} e^{-\frac{1}{2\sigma^2}(\log(m_i)-\log(M))^2} \left( \frac{1-\alpha}{M_{\max}^{1-\alpha} - M_{\min}^{1-\alpha}} \right) M^{-\alpha} \right. \\ &\quad \left. \times \left( I\{M > 4\} + \left( \frac{M-2}{2} \right) I\{2 \leq M \leq 4\} \right) dM \right\} \end{aligned} \quad (9)$$

where  $T_{\text{age}} = \tau^{-1/3} \times 10^{4/3}$  is the upper-tail mass cutoff due to aging.

## Acknowledgements

The authors thank the reviewers and associate editor for helpful comments that lead to significant improvements of this work. The authors also benefited from feedback from Ewan Cameron. Jessi Cisewski and Grant Weller were partially supported by the National Science Foundation under Grant DMS-1043903. Chad Schafer was supported by NSF Grant DMS-1106956. David W. Hogg was partially supported by the NSF (AST-0908357) and the Moore–Sloan Data Science Environment at NYU. Any opinions, findings, and conclusions or recommendations expressed in this material are those of the authors and do not necessarily reflect the views of the National Science Foundation.

## References

- Akeret, J., Refregier, A., Amara, A., Seehars, S. & Hasner, C. (2015), ‘Approximate bayesian computation for forward modeling in cosmology’, *arXiv preprint arXiv:1504.07245*.
- Ashworth, G., Fumagalli, M., Krumholz, M. R., Adamo, A., Calzetti, D., Chandar, R., Cignoni, M., Dale, D., Elmegreen, B. G., Gallagher, III, J. S., Gouliermis, D. A., Grasha, K., Grebel, E. K., Johnson, K. E., Lee, J., Tosi, M. & Wofford, A. (2017), ‘Exploring

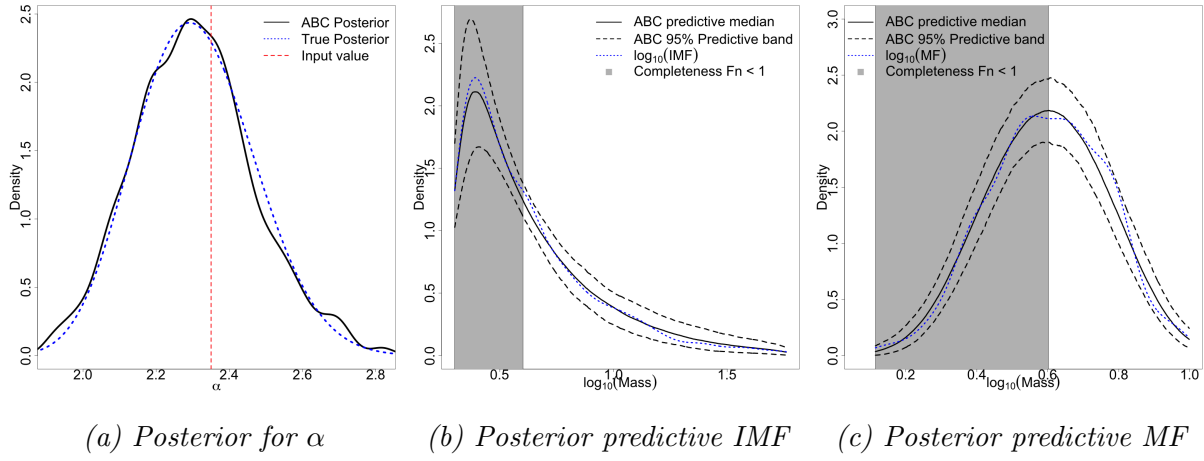


*Figure 7: Validation of summary statistics with power law model. (A) The ABC posterior for  $\alpha$  (solid black) compared to the true posterior (dotted blue) of Equation (9) using an input value of 2.35 (dashed vertical red). (B) The median of the posterior predictive IMF (solid black) with a corresponding 95% point-wise predictive band (dashed black) compared to the true IMF (blue dotted) which was simulated dataset before aging, completeness, or uncertainty were applied, and the gray shaded region indicates where the completeness function was less than 1. (C) The median of the posterior predictive MF (solid black) with a corresponding 95% point-wise predictive band (dashed black) compared to the observed MF (dotted blue) which was the simulated dataset after aging, completeness, and uncertainty were applied. For the posterior predictive IMF, 1000 draws were made from the ABC posterior of (A) and then 1000 cluster samples were drawn from the power law simulation model. For the posterior predictive MF, the 1000 cluster samples used for (B) were then put through the forward model to apply the aging, completeness, and measurement error effects.*

the IMF of star clusters: a joint SLUG and LEGUS effort’, *Monthly Notices of the Royal Astronomical Society* **469**, 2464–2480.

Bally, J. & Reipurth, B. (2005), *The Birth of Stars and Planets*, Cambridge University Press, New York.

Bastian, N., Covey, K. R. & Meyer, M. R. (2010), ‘A universal stellar initial mass function? a critical look at variations’, *Annu. Rev. Astron. Astr.* **48**, 339–389.

Bate, M. R. (2012), ‘Stellar, brown dwarf and multiple star properties from a radiation hydrodynamical simulation of star cluster formation’, *Monthly Notices of the Royal Astronomical Society* **419**(4), 3115–3146.

Beaumont, M. A., Cornuet, J.-M., Marin, J.-M. & Robert, C. P. (2009), ‘Adaptive approximate bayesian computation’, *Biometrika* **96**(4), 983–990.

Beccari, G., Petr-Gotzens, M. G., Boffin, H. M. J., Romaniello, M., Fedele, D., Carraro, G., De Marchi, G., de Wit, W.-J., Drew, J. E., Kalari, V. M., Manara, C. F., Martin, E. L., Mieske, S., Panagia, N., Testi, L., Vink, J. S., Walsh, J. R. & Wright, N. J. (2017), ‘A tale of three cities. OmegaCAM discovers multiple sequences in the color-magnitude diagram of the Orion Nebula Cluster’, *Astronomy & Astrophysics* **604**, A22.

Birrer, S., Amara, A. & Refregier, A. (2017), ‘Lensing substructure quantification in RXJ1131-1231: a 2 keV lower bound on dark matter thermal relic mass’, *Journal of Cosmology and Astroparticle Physics* **5**, 037.

Blum, M. G. (2010), ‘Approximate Bayesian computation: a nonparametric perspective’, *J. Am. Statist. Assoc.* **105**(491), 1178–1187.

Blum, M. G. & François, O. (2010), ‘Non-linear regression models for approximate Bayesian computation’, *Stat. Comput.* **20**, 63–73.

Blum, M., Nunes, M., Prangle, D. & Sisson, S. (2013), ‘A comparative review of dimension reduction methods in approximate Bayesian computation’, *Stat. Sci.* **28**(2), 189–208.

Bonnell, I. A., Clarke, C. J. & Bate, M. R. (2006), ‘The jeans mass and the origin of the knee in the imf’, *Mon. Not. R. Astron. Soc.* **368**(3), 1296–1300.

**URL:** <http://dx.doi.org/10.1111/j.1365-2966.2006.10214.x>

Cameron, E. & Pettitt, A. N. (2012), ‘Approximate bayesian computation for astronomical model analysis: a case study in galaxy demographics and morphological transformation at high redshift’, *Mon. Not. R. Astron. Soc.* **425**, 44–65.

Chabrier, G. (2005), The initial mass function: from salpeter 1955 to 2005, in ‘The Initial Mass Function 50 years later’, Springer, The Netherlands, pp. 41–50.

Chaisson, E. & McMillan, S. (2011), *Astronomy today*, 7th edn, Addison-Wesley.

Da Rio, N., Robberto, M., Hillenbrand, L. A., Henning, T. & Stassun, K. G. (2012), ‘The initial mass function of the Orion Nebula Cluster across the H-burning limit’, *Astrophys. J.* **748**(1), 1–15.

Da Rio, N., Robberto, M., Soderblom, D. R., Panagia, N., Hillenbrand, L. A., Palla, F. & Stassun, K. G. (2010), ‘A multi-color optical survey of the orion nebula cluster. ii. the hr diagram’, *The Astrophysical Journal* **722**(2), 1092.

Del Moral, P., Doucet, A. & Jasra, A. (2011), ‘An adaptive sequential Monte Carlo method for approximate Bayesian computation’, *Stat. Comput.* **22**(5), 1009–1020.

Dib, S., Schmeja, S. & Hony, S. (2017), ‘Massive stars reveal variations of the stellar initial mass function in the Milky Way stellar clusters’, *Monthly Notices of the Royal Astronomical Society* **464**, 1738–1752.

Dib, S., Shadmehri, M., Padoan, P., Maheswar, G., Ojha, D. K. & Khajenabi, F. (2010), ‘The imf of stellar clusters: effects of accretion and feedback’, *Mon. Not. R. Astron. Soc.* **405**(1), 401–420.

**URL:** <http://mnras.oxfordjournals.org/content/405/1/401.abstract>

Fearnhead, P. & Prangle, D. (2012), ‘Constructing summary statistics for approximate Bayesian computation: semi-automatic approximate Bayesian computation’, *J. Roy. Stat. Soc. B* **74**(3), 419–474.

Geha, M., Brown, T. M., Tumlinson, J., Kalirai, J. S., Simon, J. D., Kirby, E. N., Vandenberg, D. A., Muñoz, R. R., Avila, R. J., Guhathakurta, P. & Ferguson, H. C. (2013), ‘The Stellar Initial Mass Function of Ultra-faint Dwarf Galaxies: Evidence for IMF Variations with Galactic Environment’, *The Astrophysical Journal* **771**, 29.

Hahn, C., Tinker, J. L. & Wetzel, A. (2017), ‘Star Formation Quenching Timescale of Central Galaxies in a Hierarchical Universe’, *Astrophysical Journal* **841**, 6.

Hahn, C., Vakili, M., Walsh, K., Hearin, A. P., Hogg, D. W. & Campbell, D. (2017), ‘Approximate Bayesian computation in large-scale structure: constraining the galaxy-halo connection’, *Mon. Not. R. Astron. Soc.* **469**, 2791–2805.

Hansen, C. J., Kawaler, S. D. & Trimble, V. (2004), *Stellar Interiors: Physical Principles, Structure, and Evolution*, Springer, New York.

Herbel, J., Kacprzak, T., Amara, A., Refregier, A., Bruderer, C. & Nicola, A. (2017), ‘The redshift distribution of cosmological samples: a forward modeling approach’, *Journal of Cosmology and Astroparticle Physics* **8**, 035.

Hillenbrand, L. A. & Hartmann, L. W. (1998), ‘A preliminary study of the orion nebula cluster structure and dynamics’, *The Astrophysical Journal* **492**(2), 540.

**URL:** <http://stacks.iop.org/0004-637X/492/i=2/a=540>

Ishida, E., Vitenti, S., Penna-Lima, M., Cisewski, J., de Souza, R., Trindade, A., Cameron, E. et al. (2015), ‘cosmoabc: Likelihood-free inference via population monte carlo approximate bayesian computation’, *arXiv preprint arXiv:1504.06129* .

Jose, J., Herczeg, G. J., Samal, M. R., Fang, Q. & Panwar, N. (2017), ‘The Low-mass Population in the Young Cluster Stock 8: Stellar Properties and Initial Mass Function’, *The Astrophysical Journal* **836**, 98.

- Joyce, P. & Marjoram, P. (2008), ‘Approximately sufficient statistics and Bayesian computation’, *Stat. Appl. Genet. Mol.* **7**(1), 1–16.
- Kalari, V. M., Carraro, G., Evans, C. J. & Rubio, M. (2018), ‘The Magellanic Bridge cluster NGC 796: Deep optical AO imaging reveals the stellar content and initial mass function of a massive open cluster’, *ArXiv e-prints*.
- Killedar, M., Borgani, S., Fabjan, D., Dolag, K., Granato, G., Meneghetti, M., Planelles, S. & Ragone-Figueroa, C. (2018), ‘Simulation-based marginal likelihood for cluster strong lensing cosmology’, *Mon. Not. R. Astron. Soc.* **473**, 1736–1750.
- Kroupa, P. (2001), ‘On the variation of the initial mass function’, *Mon. Not. R. Astron. Soc.* **322**(2), 231–246.
- Kroupa, P., Weidner, C., Pflamm-Altenburg, J., Thies, I., Dabringhausen, J., Marks, M. & Maschberger, T. (2012), The stellar and sub-stellar IMF of simple and composite populations, in I. Oswalt, T. D. with McLean, H. Bond, L. French, P. Kalas, M. Barstow, G. Gilmore & W. Keel, eds, ‘Stellar Systems and Galactic Structure’, Vol. 5 of *Planets, Stars, and Stellar Systems*, Springer, Dordrecht, pp. 115–142.
- Li, H., Gnedin, O. Y., Gnedin, N. Y., Meng, X., Semenov, V. A. & Kravtsov, A. V. (2017), ‘Star Cluster Formation in Cosmological Simulations. I. Properties of Young Clusters’, *The Astrophysical Journal* **834**, 69.
- Lim, B., Chun, M.-Y., Sung, H., Park, B.-G., Lee, J.-J., Sohn, S. T., Hur, H. & Bessell, M. S. (2013), ‘The starburst cluster Westerlund 1: the initial mass function and mass segregation’, *Astron. J.* **145**, 46–64.
- Lin, C.-A. & Kilbinger, M. (2015), ‘A new model to predict weak-lensing peak counts. II. Parameter constraint strategies’, *Astronomy & Astrophysics* **583**, A70.
- Marin, J.-M., Pudlo, P., Robert, C. P. & Ryder, R. J. (2012), ‘Approximate bayesian computational methods’, *Statistics and Computing* **22**(6), 1167–1180.

- Marjoram, P., Molitor, J., Plagnol, V. & Tavaré, S. (2003), ‘Markov chain Monte Carlo without likelihoods’, *P. Natl. Acad. Sci. USA* **100**(26), 15324–15328.
- Massey, P. (2003), ‘Massive stars in the local group: implications for stellar evolution and star formation’, *Annu. Rev. Astron. Astr.* **41**, 15–56.
- McMillan, P. J. (2016), ‘The mass distribution and gravitational potential of the milky way’, *Monthly Notices of the Royal Astronomical Society* p. stw2759.
- Mitzenmacher, M. (2004), ‘A brief history of generative models for power law and lognormal distributions’, *Internet mathematics* **1**(2), 226–251.
- Offner, S. S., Clark, P. C., Hennebelle, P., Bastian, N., Bate, M. R., Hopkins, P. F., Moraux, E. & Whitworth, A. P. (2014), ‘The origin and universality of the stellar initial mass function’, *Protostars and Planets VI* **1**, 53–75.
- Parker, A. H. (2015), ‘The intrinsic neptune trojan orbit distribution: Implications for the primordial disk and planet migration’, *Icarus* **247**, 112–125.
- Peel, A., Lin, C.-A., Lanusse, F., Leonard, A., Starck, J.-L. & Kilbinger, M. (2017), ‘Cosmological constraints with weak-lensing peak counts and second-order statistics in a large-field survey’, *Astronomy & Astrophysics* **599**, A79.
- Pritchard, J. K., Seielstad, M. T. & Perez-Lezaun, A. (1999), ‘Population growth of human Y chromosomes: A study of Y chromosome microsatellites’, *Mol. Bio. Evol.* **16**(12), 1791–1798.
- Robin, A., Reylé, C., Fliri, J., Czekaj, M., Robert, C. & Martins, A. (2014), ‘Constraining the thick disc formation scenario of the milky way’, *Astronomy & Astrophysics* **569**, A13.
- Salpeter, E. E. (1955), ‘The luminosity function and stellar evolution’, *Astrophys. J.* **121**, 161–167.
- Schafer, C. M. & Freeman, P. E. (2012), Likelihood-free inference in cosmology: potential for the estimation of luminosity functions, in ‘Statistical Challenges in Modern Astronomy V’, Springer, New York, pp. 3–19.

- Shetty, S. & Cappellari, M. (2014), ‘Salpeter normalization of the stellar initial mass function for massive galaxies at  $z \sim 1$ ’, *Astrophys. J. Let.* **786**, L10.
- Simon, H. A. (1955), ‘On a class of skew distribution functions’, *Biometrika* **42**(314), 425–440.
- Sisson, S. A., Fan, Y. & Tanaka, M. M. (2007), ‘Sequential Monte Carlo without likelihoods’, *P. Natl. Acad. Sci. USA* **104**(6), 1760–1765.
- Spiniello, C., Trager, S., Koopmans, L. V. E. & Conroy, C. (2014), ‘The stellar IMF in early-type galaxies from a non-degenerate set of optical line indices’, *Mon. Not. R. Astron. Soc.* **438**, 1483–1499.
- Tavaré, S., Balding, D. J., Griffiths, R. & Donnelly, P. (1997), ‘Inferring coalescence times from DNA sequence data’, *Genetics* **145**, 505–518.
- Treu, T., Auger, M. W., Koopmans, L. V. E., Gavazzi, R., Marshall, P. J. & Bolton, A. S. (2010), ‘The initial mass function of early-type galaxies’, *Astrophys. J.* **709**, 1195–1202.
- Weisz, D. R., Fouesneau, M., Hogg, D. W., Rix, H.-W., Dolphin, A. E., Dalcanton, J. J., Foreman-Mackey, D. T., Lang, D., Johnson, L. C., Beerman, L. C. et al. (2013), ‘The Panchromatic Hubble Andromeda Treasury IV. A probabilistic approach to inferring the high-mass stellar initial mass function and other power-law functions’, *Astrophys. J.* **762**(2), 123–143.
- Weyant, A., Schafer, C. & Wood-Vasey, W. M. (2013), ‘Likelihood-free cosmological inference with type Ia supernovae: approximate Bayesian computation for a complete treatment of uncertainty’, *Astrophys. J.* **764**, 116–130.
- Woosley, S. E. & Heger, A. (2015), The Deaths of Very Massive Stars, in J. S. Vink, ed., ‘Very Massive Stars in the Local Universe’, Vol. 412 of *Astrophysics and Space Science Library*, p. 199.

**Data:** Observed stellar masses,  $(m_{\text{obs}})$

**Result:** ABC posterior sample of  $\theta$

At iteration  $t = 1$ :

**for**  $j = 1, \dots, kN$  **do**

    Propose  $\theta_t^{(j)}$  by drawing  $\theta_t^* \sim \pi(\theta)$

    Generate cluster stellar masses  $m_{\text{sim}}$  from  $F(m | \theta_t^*)$

    Calculate distance  $\rho_t^{(j)} \leftarrow \rho(m_{\text{sim}}, m_{\text{obs}})$

**end**

$\theta_t^{(j)} \leftarrow \theta_t^{(l)}, l = \text{index of } N \text{ smallest } \rho_t^{(q)}, q = 1, \dots, kN$

$W_t^{(j)} \leftarrow 1/N, j = 1, \dots, N$

At iterations  $t = 2, \dots, T$ :

**for**  $j = 1, \dots, N$  **do**

**while**  $\rho(m_{\text{sim}}, m_{\text{obs}}) > \epsilon_t$  **do**

        Select  $\theta^{(j)}$  by drawing from the  $\theta_{t-1}^{(i)}$  with probabilities  $W_{t-1}^{(i)}, i = 1, \dots, N$

        Generate  $\theta^{*(j)}$  from transition kernel  $K(\theta^{(j)}, \cdot)$

        Generate cluster stellar masses  $m_{\text{sim}}$  from  $F(m | \theta^{*(j)})$

**end**

$\theta_t^{(j)} \leftarrow \theta^{*(j)}$

$W_t^{(j)} \leftarrow \frac{\pi(\theta_t^{(j)})}{\sum_{i=1}^N W_{t-1}^{(i)} K(\theta_{t-1}^{(i)}, \theta_t^{(j)})}$

**end**

$W_t^{(j)} \leftarrow \frac{W_t^{(j)}}{\sum_{l=1}^N W_t^{(l)}}, j = 1, \dots, N$

**Algorithm 1:** Stellar IMF ABC algorithm with sequential sampling

Number	$\lambda^{-1}$	$\alpha$	$\gamma$	$M_{\text{tot}}$	$n_{\text{obs}}$
1	0.25	0.3	0.5	1000	1166
2	0.25	0.3	1.0	1000	1142
3	0.25	0.3	1.5	1000	1148
4	0.25	0.7	0.5	1000	2801
5	0.25	0.7	1.0	1000	2698
6	0.25	0.7	1.5	1000	2710

Table 1: Parameter values for the simulation study and the number of stars in the data set,  $n_{\text{obs}}$ . Figure 3: The simulated IMF's used as the observations in the simulation study displayed as number of stars by  $\log_{10}$  mass.

